J|A|C|S ARTICLES

Published on Web 01/21/2009

Intramolecular Electron-Transfer Rates in Mixed-Valence Triarylamines: Measurement by Variable-Temperature ESR Spectroscopy and Comparison with Optical Data

Kelly Lancaster,[†] Susan A. Odom,[†] Simon C. Jones,[†,‡] S. Thayumanavan,[‡] Seth R. Marder,[†,‡] Jean-Luc Brédas,[†] Veaceslav Coropceanu,[*,†] and Stephen Barlow[*,†,‡]

School of Chemistry and Biochemistry and Center for Organic Photonics and Electronics, Georgia Institute of Technology, Atlanta, Georgia 30332-0400, and Department of Chemistry, University of Arizona, Tucson, Arizona 85721

Received October 28, 2008; E-mail: coropceanu@gatech.edu; stephen.barlow@chemistry.gatech.edu

Abstract: The electron spin resonance spectra of the radical cations of 4,4′-bis[di(4-methoxyphenyl)amino]tolane, *E*-4,4′-bis[di(4-methoxyphenyl)amino]stilbene, and *E,E*-1,4-bis{4-[di(4-methoxyphenyl)amino]styryl}-benzene in dichloromethane exhibit five lines over a wide temperature range due to equivalent coupling to two ^{14}N nuclei, indicating either delocalization between both nitrogen atoms or rapid intramolecular electron transfer on the electron spin resonance time scale. In contrast, those of the radical cations of 1,4-bis{4-[di(4-methoxyphenyl)amino]phenylethynyl}benzene and *E,E*-1,4-bis{4-[di(4-*n*-butoxyphenyl)amino]styryl}-2,5-dicyanobenzene exhibit line shapes that vary strongly with temperature, displaying five lines at room temperature and only three lines at ca. 190 K, indicative of slow electron transfer on the electron spin resonance time scale at low temperatures. The rates of intramolecular electron transfer in the latter compounds were obtained by simulation of the electron spin resonance spectra and display an Arrhenius temperature dependence. The activation barriers obtained from Arrhenius plots are significantly less than anticipated from Hush analyses of the intervalence bands when the diabatic electron-transfer distance, *R*, is equated to the N—N distance. Comparison of optical and electron spin resonance data suggests that *R* is in fact only ca. 40% of the N—N distance, while the Arrhenius prefactor indicates that the electron transfer falls in the adiabatic regime.

Introduction

Mixed-valence (MV) compounds contain two or more linked redox centers in different formal oxidation states and are among the simplest model systems for the study of electron-transfer (ET) and (de)localization phenomena. The interplay between the electronic coupling (V) and the reorganization energy (λ) in a MV compound determines whether the system belongs to Robin and Day's class II (i.e., is valence-localized) or class III (valence-delocalized)[1] and, in the former case, influences the rate of intramolecular ET. The work of Hush links optical and thermal intramolecular ET for class-II MV compounds.[2] Both V and λ can be obtained from an analysis of the intervalence charge-transfer (IVCT) band associated with optical intramolecular ET. In the semiclassical formalism,

$$\lambda = E_{op} \tag{1}$$

where E_{op} is the energy of the IVCT band maximum, while V is given by:

$$V = \frac{\mu_{ge} E_{op}}{eR} \tag{2}$$

where μ_{ge} is the transition dipole moment of the IVCT band and R is the diabatic ET distance.[2] While μ_{ge} and E_{op} are accessible from optical measurements, R cannot be directly measured and can only be obtained indirectly from μ_{ge} and the adiabatic dipole moment shift.[3,4] R, which can be considered as the distance between the redox centers in the absence of electronic coupling, is often simply equated to the metal–metal separation in inorganic systems, although this ignores the possibility that the redox center may have some mixed metal and bridge character. Estimates of V from eq 2 are particularly problematic for organic MV compounds where, in addition to the possibility of delocalization of the diabatic states into the bridge, the centers of multiatom redox sites can themselves be difficult to define.

At the same time, determination of the activation barrier (ΔG^*) associated with thermal intramolecular ET can also afford insight into the microscopic parameters:[5]

$$\Delta G^* = \frac{(\lambda - 2V)^2}{4\lambda} \tag{3}$$

The barrier can be obtained from variable-temperature (VT) spectroscopic measurements of the ET rate. Depending on the

[†] Georgia Tech.
[‡] University of Arizona.

(1) Robin, M. B.; Day, P. *Adv. Inorg. Chem. Radiochem.* **1967**, *10*, 247.
(2) Hush, N. S. *Prog. Inorg. Chem.* **1967**, *8*, 391.
(3) Cave, R. J.; Newton, M. D. *Chem. Phys. Lett.* **1996**, *249*, 15.
(4) The dipole moment shift can be obtained from Stark-effect experiments or from quantum-mechanical calculations.
(5) Sutin, N. *Prog. Inorg. Chem.* **1983**, *30*, 441.

Chart 1

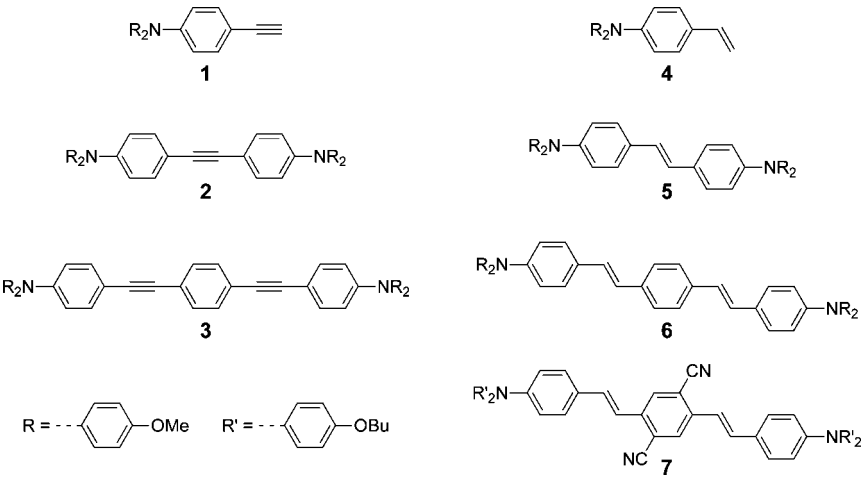

magnitude of the rates and the chemical nature of the system in question, appropriate spectroscopic tools can include Mössbauer, nuclear magnetic resonance, infrared, and electron spin resonance (ESR) spectroscopy.[6] VT-ESR, in particular, has been widely used for measuring ET rates and activation barriers in organic MV systems.[7−16]

Triarylamine-based radical cations have recently emerged as an important class of organic MV compounds, due in part to the role played by bis(triarylamine)s as hole-transport materials in organic electronic applications.[17−20] Although optical ET has been extensively studied in bis(triarylamine) MV cations,[21−42] we are aware of only one determination of *thermal* intramolecular ET rates in such compounds: VT-ESR was used to measure ET rates for an example with a spiro Si linkage, but the absence of an IVCT band in the expected near-IR region precluded comparison with optical estimates of V and λ.[43,44] VT-ESR has also been employed to study *inter*molecular ET in solutions containing 4,4′-bis[(phenyl)(*m*-tolyl)amino]biphenyl] and its class-III radical cation.[45] However, most ESR studies of MV bis(triarylamine)s to date have generally been restricted to room-temperature spectra of species that appear delocalized on the ESR time scale, i.e., that exhibit spectra in the fast limit with equivalent coupling of the unpaired electron to both nitrogen centers due to either static delocalization in class-III cations or to rapid intramolecular ET in class-II species.[35−38,46,47] Single-temperature spectra have also been reported for several systems with more than two amine redox centers.[48−51]

Here we report an ESR study of the triarylamine radical cations $\mathbf{1}^+$−$\mathbf{3}^+$ and $\mathbf{5}^+$−$\mathbf{7}^+$, while an additional model compound, $\mathbf{4}^+$, is studied only computationally (Chart 1). In particular, the magnitudes of V, λ, and the hyperfine interactions in $\mathbf{3}^+$ and $\mathbf{7}^+$ allow one to observe transitions from slow to fast ET regimes on the ESR time scale as a function of temperature. The well-resolved IVCT bands of $\mathbf{3}^+$ and $\mathbf{7}^+$ also permit estimates of the microscopic parameters using eqs 1 and 2, thus allowing the first comparison of thermal and optical ET in bis(triarylamine) MV compounds.

Results and Discussion

Compounds **1**−**3**, **5**, and **6** were synthesized as described in the literature.[24,25,37,38] The new compound **7**[52] was synthesized under typical Horner−Emmons conditions[53,54] from 4-[bis(4-*n*-butoxyphenyl)amino]benzaldehyde (**8**) and tetraethyl-(2,5-

(6) Richardson, D. E. *Comments Inorg. Chem.* **1985**, *3*, 367.
(7) Nelsen, S. F.; Ramm, M. T.; Wolff, J. J.; Powell, D. R. *J. Am. Chem. Soc.* **1997**, *119*, 6836.
(8) Nelsen, S. F.; Ismagilov, R. F.; Powell, D. R. *J. Am. Chem. Soc.* **1997**, *119*, 10213.
(9) Nelsen, S. F.; Trieber, D. A.; Wolff, J. J.; Powell, D. R.; Rogers-Crowley, S. *J. Am. Chem. Soc.* **1997**, *119*, 6873.
(10) Rak, S. F.; Miller, L. L. *J. Am. Chem. Soc.* **1992**, *114*, 1388.
(11) Bonvoisin, J.; Launay, J.-P.; Rovira, C.; Veciana, J. *Angew. Chem., Int. Ed. Engl.* **1994**, *33*, 2106.
(12) Nelsen, S. F.; Ismagilov, R. F.; Trieber, D. A. *Science* **1997**, *278*, 846.
(13) Lindeman, S. V.; Rosokha, S. V.; Sun, D.; Kochi, J. K. *J. Am. Chem. Soc.* **2002**, *124*, 843.
(14) Rosokha, S. V.; Sun, D.-L.; Kochi, J. K. *J. Phys. Chem. A* **2002**, *106*, 2283.
(15) Sun, D.; Rosokha, S. V.; Kochi, J. K. *J. Am. Chem. Soc.* **2004**, *126*, 1388.
(16) Rovira, C.; Ruiz-Molina, D.; Elsner, O.; Vidal-Gancedo, J.; Bonvoisin, J.; Launay, J.-P.; Veciana, J. *Chem. Eur. J.* **2001**, *7*, 240.
(17) Tang, C. W.; Van Slyke, S. A. *Appl. Phys. Lett.* **1987**, *51*, 913.
(18) Bulovic, V.; Gu, G.; Burrows, P. E.; Forrest, S. R.; Thompson, M. E. *Nature* **1996**, *380*, 29.
(19) Kido, J.; Kimura, M.; Nagai, K. *Science* **1995**, *267*, 1332.
(20) Borsenberger, P. M.; Weiss, D. S. *Organic Photoreceptors for Xerography*; Marcel Dekker: New York, 1998.
(21) Bonvoisin, J.; Launay, J.-P.; Van der Auweraer, M.; De Schryver, F. C. *J. Phys. Chem.* **1994**, *98*, 5052.
(22) Bonvoisin, J.; Launay, J.-P.; Verbouwe, W.; Van der Auweraer, M.; De Schryver, F. C. *J. Phys. Chem.* **1996**, *100*, 17079.
(23) Lambert, C.; Nöll, G. *Angew. Chem., Int. Ed.* **1998**, *37*, 2107.
(24) Lambert, C.; Nöll, G.; Schmälzlin, E.; Meerholz, K.; Bräuchle, C. *Chem. Eur. J.* **1998**, *4*, 2129.
(25) Lambert, C.; Nöll, G. *J. Am. Chem. Soc.* **1999**, *121*, 8434.
(26) Lambert, C.; Nöll, G.; Hampel, F. *J. Phys. Chem. A* **2001**, *105*, 7751.
(27) Lambert, C.; Nöll, G.; Schelter, J. *Nat. Mater.* **2002**, *1*, 69.
(28) Lambert, C.; Nöll, G. *Chem. Eur. J.* **2002**, *8*, 3467.
(29) Coropceanu, V.; Malagoli, M.; André, J. M.; Brédas, J. L. *J. Chem. Phys.* **2001**, *115*, 10409.
(30) Coropceanu, V.; Malagoli, M.; André, J. M.; Brédas, J. L. *J. Am. Chem. Soc.* **2002**, *124*, 10519.
(31) Coropceanu, V.; Lambert, C.; Nöll, G.; Brédas, J. L. *Chem. Phys. Lett.* **2003**, *373*, 153.
(32) Low, P. J.; Paterson, M. A. J.; Puschmann, H.; Goeta, A. E.; Howard, J. A. K.; Lambert, C.; Cherryman, J. C.; Tackley, D. R.; Leeming, S.; Brown, B. *Chem. Eur. J.* **2004**, *10*, 83.
(33) Lambert, C.; Amthor, S.; Schelter, J. *J. Phys. Chem. A* **2004**, *108*, 6474.
(34) Szeghalmi, A. V.; Erdmann, M.; Engel, V.; Schmitt, M.; Amthor, S.; Kriegisch, V.; Nöll, G.; Stahl, R.; Lambert, C.; Leusser, D.; Stalke, D.; Zabel, M.; Popp, J. *J. Am. Chem. Soc.* **2004**, *126*, 7834.
(35) Jones, S. C.; Coropceanu, V.; Barlow, S.; Kinnibrugh, T.; Timofeeva, T.; Brédas, J.-L.; Marder, S. R. *J. Am. Chem. Soc.* **2004**, *126*, 11782.
(36) Lambert, C.; Risko, C.; Coropceanu, V.; Schelter, J.; Amthor, S.; Gruhn, N. E.; Durivage, J. C.; Brédas, J. L. *J. Am. Chem. Soc.* **2005**, *127*, 8508.

Scheme 1

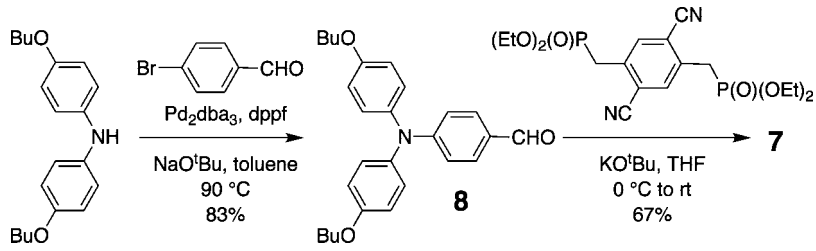

dicyano-α,α′-*p*-xylylenediphosphonate),[55] as shown in Scheme 1. Compound **8** was synthesized via a Buchwald−Hartwig-type coupling[56,57] of 4-bromobenzaldehyde and di(4-*n*-butoxyphenyl)amine.[47] As in several of our previous studies of oxidized amine cations,[35,37,38,47,58−60] radical cations were generated by chemical oxidation of the neutral species in dichloromethane using tris(4-bromophenyl)aminium hexachloroantimonate; oxidant/neutral ratios of ca. 1:10 were used to minimize disproportionation to dications which, at least in some cases, are known or are anticipated to also give an ESR signal.[38]

Room-temperature ESR spectra of the radical cations are shown in Figure 1 and, consistent with previous studies of mixtures of 4,4′-bis[(phenyl)(*m*-tolyl)amino]biphenyl and its radical cation at similar concentrations,[45] appear to be unaffected by *inter*molecular ET between neutral and cationic species. Some of the VT-ESR spectra (those for $\mathbf{2}^+$ and $\mathbf{6}^+$), which were collected at higher concentrations, are, however, somewhat narrowed by intermolecular ET (see Supporting Information). The ESR spectra of $\mathbf{3}^+$ and $\mathbf{7}^+$ show significant temperature dependence (Figures 2 and 3) while the low-temperature (ca. 180 K) spectra of $\mathbf{2}^+$, $\mathbf{5}^+$, and $\mathbf{6}^+$ are essentially the same as the respective room-temperature spectra in Figure 1.

As shown in Figure 2, the low-temperature three-line ESR spectrum of $\mathbf{3}^+$ is nearly identical to the room-temperature spectrum of $\mathbf{1}^+$, consistent with coupling of the unpaired electron to a single ^{14}N ($I = 1$) nucleus, i.e., with slow intramolecular ET on the ESR time scale.[61] As the temperature is increased, a transition to a five-line pattern is observed, consistent with an increase in the rate of thermal intramolecular ET. The same pattern emerges for $\mathbf{7}^+$ (Figure 3), although the three-line low-temperature ESR spectrum is still affected by intramolecular ET and so does not correspond to the slow limit.

The VT-ESR spectra of $\mathbf{3}^+$ and $\mathbf{7}^+$ were simulated using the ESR-EXN program in order to obtain intramolecular ET rates[62,63] (Figures 2 and 3; see Supporting Information for details). Hyperfine coupling constants for $\mathbf{1}^+$ and $\mathbf{4}^+$ were computed with density functional theory (DFT) to model the instantaneous localization of charge on one triarylamine. The constants were taken as initial inputs for $\mathbf{3}^+$ and $\mathbf{7}^+$, respectively, and then adjusted, along with the line width and exchange rate, to obtain the best fit to each experimental spectrum. Based on the DFT calculations, hyperfine interactions with one ^{14}N ($I = 1$) nucleus and six or seven ^1H ($I = 1/2$) nuclei were included in the simulations for $\mathbf{3}^+$ or $\mathbf{7}^+$, respectively. The simulations yield ET rates, k_{ET}, that change from ca. 10^7 s^{-1} at low temperature to ca. 10^8 s^{-1} at room temperature with $a_N = 8.4$ G. Although the room-temperature ESR spectra for $\mathbf{3}^+$ and $\mathbf{7}^+$ exhibit five lines, the line shapes do not correspond to those for the fast limit in which the triarylamine centers are equivalent

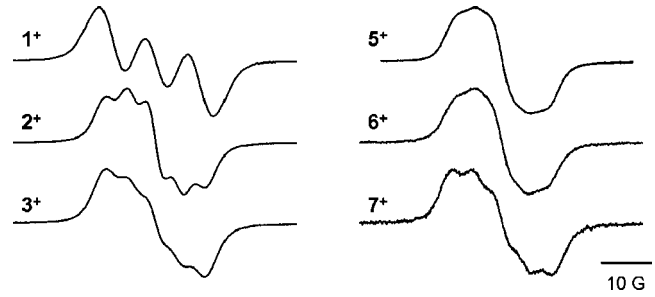

Figure 1. Room-temperature ESR spectra of $\mathbf{1}^+$−$\mathbf{3}^+$ and $\mathbf{5}^+$−$\mathbf{7}^+$ in CH_2Cl_2 obtained upon chemical oxidation with $[(p\text{-}BrC_6H_4)_3N]^+[SbCl_6]^-$.

(37) Barlow, S.; Risko, C.; Coropceanu, V.; Tucker, N. M.; Jones, S. C.; Levi, Z.; Khrustalev, V. N.; Antipin, M. Y.; Kinnibrugh, T. L.; Timofeeva, T.; Marder, S. R.; Brédas, J. L. *Chem. Commun.* **2005**, 764.
(38) Barlow, S.; Risko, C.; Chung, S.-J.; Tucker, N. M.; Coropceanu, V.; Jones, S. C.; Levi, Z.; Brédas, J. L.; Marder, S. R. *J. Am. Chem. Soc.* **2005**, *127*, 16900.
(39) Nöll, G.; Avola, M. *J. Phys. Org. Chem.* **2006**, *19*, 238.
(40) Nöll, G.; Avola, M.; Lynch, M.; Daub, J. *J. Phys. Chem. C* **2007**, *111*, 3197.
(41) Amthor, S.; Lambert, C. *J. Phys. Chem. A* **2006**, *110*, 1177.
(42) Nöll, G.; Amthor, S.; Avola, M.; Lambert, C.; Daubl, J. *J. Phys. Chem.* **2007**, *111*, 3512.
(43) Hirao, Y.; Urabe, M.; Ito, A.; Tanaka, K. *Angew. Chem., Int. Ed.* **2007**, *46*, 3300.
(44) Five-line spectra were observed at all temperatures, indicative of rapid ET; however, simulation of the temperature-dependent line shapes yielded ET rates. Although these data were interpreted using an Eyring plot, they can also be satisfactorily fit to an Arrhenius expression to give a prefactor of ca. 3×10^{12} s^{-1} and a barrier of 1300 cm^{-1}.
(45) Veregin, R. P.; Harbour, J. R. *J. Phys. Chem.* **1990**, *94*, 6231.
(46) Rohde, D.; Dunsch, L.; Tabet, A.; Hartmann, H.; Fabian, J. *J. Phys. Chem. B* **2006**, *110*, 8223.
(47) Odom, S. A.; Lancaster, K.; Beverina, L.; Lefler, K. M.; Thompson, N. J.; Coropceanu, V.; Brédas, J.-L.; Marder, S. R.; Barlow, S. *Chem. Eur. J.* **2007**, *13*, 9637.
(48) Fáber, R.; Mielke, G. F.; Rapta, P.; Stašo, A.; Nuyken, O. *Collect. Czech. Chem. Commun.* **2000**, *65*, 1403.
(49) Yan, X. Z.; Pawlas, J.; Goodson, T.; Hartwig, J. F. *J. Am. Chem. Soc.* **2005**, *127*, 9105.
(50) Rapta, P.; Tabet, A.; Hartmann, H.; Dunsch, L. *J. Mater. Chem.* **2007**, *17*, 4998.
(51) Stickley, K. R.; Blackstock, S. C. *Tetrahedron Lett.* **1995**, *36*, 1585.
(52) Since cyanoarenes are often poorly soluble in solvents such as CH_2Cl_2, compound **7** was synthesized with the electronically similar, but more solubilizing, BuO groups in place of the MeO groups used for compounds **1**−**6**.
(53) Horner, L.; Hoffmann, H.; Wippel, H. G. *Chem. Ber.* **1958**, *91*, 61.
(54) Wadsworth, W. S.; Emmons, W. D. *J. Am. Chem. Soc.* **1961**, *83*, 1733.
(55) Wenseleers, W.; Stellacci, F.; Meyer-Friedrichsen, T.; Mangel, T.; Bauer, C. A.; Pond, S. J. K.; Marder, S. R.; Perry, J. W. *J. Phys. Chem. B.* **2002**, *106*, 6853.
(56) Wolfe, J. P.; Wagaw, S.; Buchwald, S. L. *J. Am. Chem. Soc.* **1996**, *118*, 7215.
(57) Driver, M. S.; Hartwig, J. F. *J. Am. Chem. Soc.* **1996**, *118*, 7217.
(58) Coropceanu, V.; Gruhn, N. E.; Barlow, S.; Lambert, C.; Durivage, J. C.; Bill, T. G.; Nöll, G.; Marder, S. R.; Brédas, J.-L. *J. Am. Chem. Soc.* **2004**, *126*, 2727.
(59) Zheng, S.; Barlow, S.; Risko, C.; Kinnibrugh, T. L.; Khrustalev, V. N.; Antipin, M. Y.; Tucker, N. M.; Timofeeva, T.; Coropceanu, V.; Jones, S. C.; Brédas, J.-L.; Marder, S. R. *J. Am. Chem. Soc.* **2006**, *128*, 1812.
(60) Risko, C.; Coropceanu, V.; Barlow, S.; Geskin, V.; Schmidt, K.; Gruhn, N. E.; Marder, S. R.; Brédas, J.-L. *J. Phys. Chem. C* **2008**, *112*, 7959.

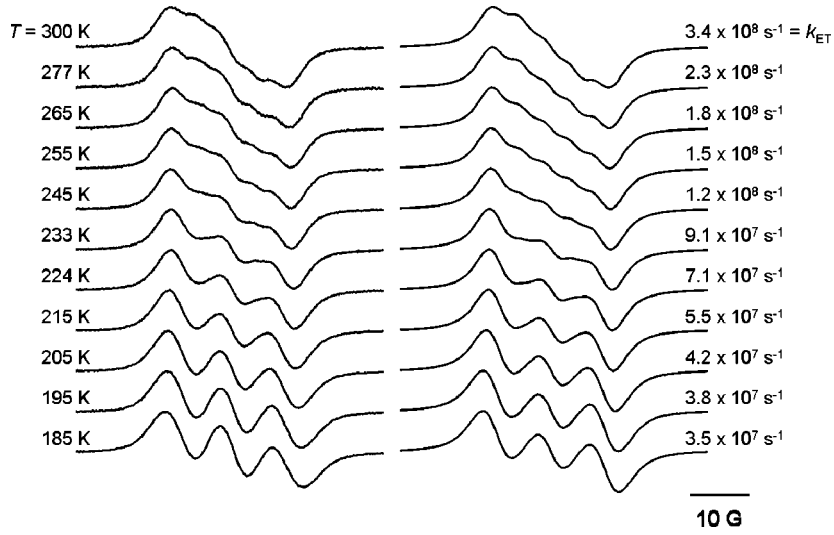

Figure 2. VT-ESR spectra for $\mathbf{3}^+$ (left) and simulated spectra (right) with derived intramolecular ET rates.

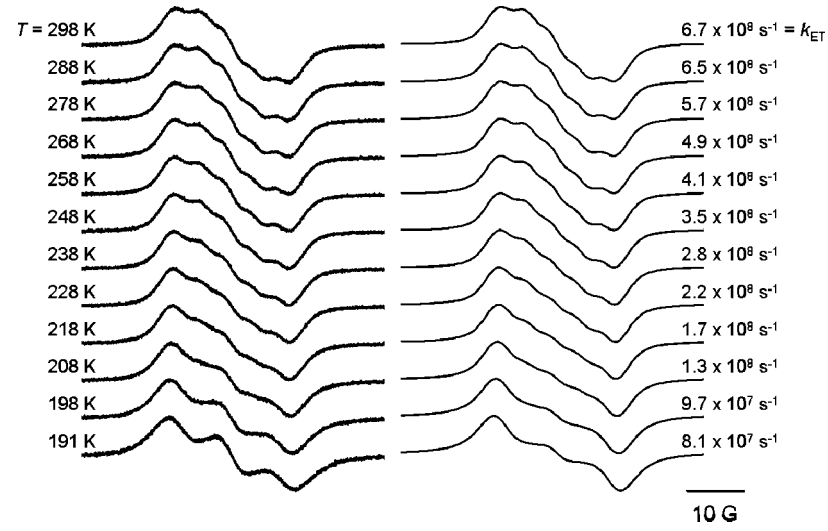

Figure 3. VT-ESR spectra for $\mathbf{7}^+$ (left) and simulated spectra (right) with derived intramolecular ET rates.

on the ESR time scale; simulations with $k_{ET} > 10^{10}$ s^{-1} indicate that in that case the height of the second peak in the first-derivative ESR spectrum would exceed that of the first peak.

The room-temperature ESR spectra of $\mathbf{2}^+$, $\mathbf{5}^+$, and $\mathbf{6}^+$ (Figure 1) are quite similar to one another, although those of $\mathbf{5}^+$ and $\mathbf{6}^+$ are somewhat less well-resolved than that of $\mathbf{2}^+$ due to hyperfine coupling to the additional ^{1}H nuclei of the vinylene groups. In contrast to the room-temperature ESR spectra of $\mathbf{3}^+$ and $\mathbf{7}^+$, where the outer peaks of the first-derivative spectrum are the most intense, the second peaks are more intense in the spectra of $\mathbf{2}^+$, $\mathbf{5}^+$, and $\mathbf{6}^+$, consistent with ET in the fast limit on the ESR time scale. These spectra can be simulated equally well assuming either rapid intramolecular ET between two nitrogen centers with $a_N(1 \times N) \approx 8$ G and $k_{ET} > 10^{10}$ s^{-1} or a static delocalization with $a_N(2 \times N) \approx 4$ G (see Supporting Information).

The observation of ET rates $< 10^9$ s^{-1} in the room-temperature ESR spectrum of the phenylene-ethynylene species $\mathbf{3}^+$, while its phenylene-vinylene analogue $\mathbf{6}^+$ shows fast-limit ESR spectra at all temperatures examined, is qualitatively consistent with analyses of IVCT bands, which indicate stronger coupling and lower reorganization energies in vinylene-bridged species than in their ethynylene analogues.[38] The fast-limit ESR spectra of the shorter compounds $\mathbf{2}^+$ and $\mathbf{5}^+$ are also consistent with the larger V (and, in the case of $\mathbf{2}^+$ vs $\mathbf{3}^+$, lower λ) values previously estimated from IVCT data;[25,37,38] indeed, IVCT line shape and solvatochromism, crystallography, and vibrational spectra suggest that $\mathbf{5}^+$ is statically delocalized, i.e., that it belongs to Robin and Day's class III.[37,38] The qualitative differences in ESR behavior between $\mathbf{6}^+$ and $\mathbf{7}^+$, which both have phenylene-vinylene bridges of the same length, are again consistent with the trends in coupling and reorganization energy implied by their IVCT bands (see ref 38 for IVCT data for $\mathbf{6}^+$; see Figure 5 and Table 1 for $\mathbf{7}^+$). The reduced V in $\mathbf{7}^+$ can be attributed to

(61) The a_N values obtained (8.2 G for $\mathbf{1}^+$; 8.4 G for the room-temperature spectra of $\mathbf{3}^+$ and $\mathbf{7}^+$) may be compared to a value of 8.97 G previously reported for the tris(4-methoxyphenyl)aminium ion in acetonitrile (Seo, E. T.; Nelson, R. F.; Fritsch, J. M.; Marcoux, L. S.; Leedy, D. W.; Adams, R. N. *J. Am. Chem. Soc.* **1966**, *88*, 3498).
(62) Heinzer, J. *Mol. Phys.* **1971**, *22*, 167.
(63) Heinzer, J. Quantum Chemistry Program Exchange, *No. 209*, 1972.
(64) Although an Eyring analysis was used in ref 11, the published VT-ESR data can also be fitted to an Arrhenius expression to give a barrier of 1130 cm^{-1}, while a value of 1470 cm^{-1} is obtained by analysis of the IVCT band, if R is equated to the separation between the central carbons of the triarylmethyl groups.

Table 1. Comparison of Optical and Thermal Electron-Transfer Parameters for $\mathbf{3}^+$ and $\mathbf{7}^+$

		IVCT				ESR			
	λ^a/cm^{-1}	$\mu_{ge}{}^b$/D	$R_{NN}{}^c$/Å	$V_{NN}{}^d$/cm^{-1}	$\Delta G^{\ddagger}_{NN}{}^e$/cm^{-1}	$\Delta G^{\ddagger}_{ESR}{}^f$/cm^{-1}	$V_{ESR}{}^g$/cm^{-1}	$R_{ESR}{}^h$/Å	$A_{ESR}{}^f$/s^{-1}
$\mathbf{3}^+$	7780[i]	5.85	19.45	490[i]	1490	940	1180	8.0	3.1×10^{10}
$\mathbf{7}^+$	7450	5.78	19.03	470	1420	840	1220	7.4	4.4×10^{10}

[a] Obtained from eq 1. [b] Obtained from Gaussian fits of the IVCT bands using $\mu_{ge} = 0.9584(\int \varepsilon\, dE/E_{op})^{0.5}$ where ε is in M^{-1} cm^{-1} and E is in cm^{-1}.[65] [c] Obtained from DFT optimizations of the neutral compounds. [d] Obtained from eq 2 using E_{op}, μ_{ge}, and R_{NN}. [e] Obtained from eq 3 using the IVCT estimates of λ and V_{NN}. [f] Obtained from the fits of the VT rate data to eq 4. [g] Obtained from eq 3 using $\Delta G^{\ddagger}_{ESR}$ and the IVCT value of λ. [h] Obtained from eq 2 using V_{ESR} and the IVCT values of μ_{ge} and E_{op}. [i] From ref 38; similar values can be found in refs 25 (in the presence of electrolyte) and 27.

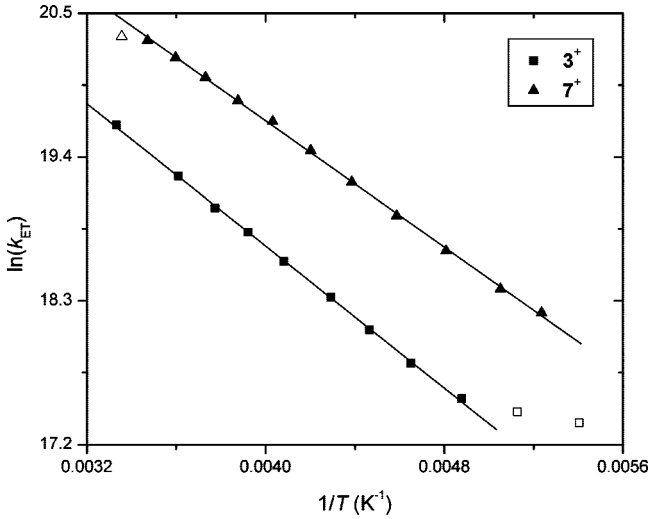

Figure 4. Arrhenius plots of the thermal intramolecular ET rates from Figures 2 and 3. Rates represented by open symbols were excluded from the linear fits since simulations of the ESR spectra approaching either the slow or fast limit (low- and high-temperature data for $\mathbf{3}^+$ and $\mathbf{7}^+$, respectively) are rather insensitive to k_{ET}.

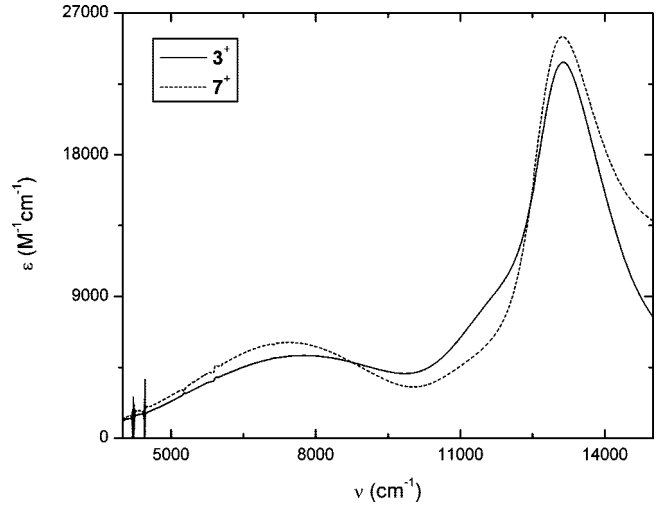

Figure 5. Visible-NIR absorption spectra of $\mathbf{3}^+$ and $\mathbf{7}^+$ in dichloromethane obtained by oxidation of an excess of the corresponding neutral species with tris(4-bromophenyl)aminium hexachloroantimonate. The low-energy bands, with maxima at 7780 and 7450 cm^{-1} for $\mathbf{3}^+$ and $\mathbf{7}^+$, respectively, are assigned as IVCT bands.[65]

a lowering of the energy of the bridge-based orbitals that mediate the coupling between the triarylamine-based orbitals by the electron-withdrawing cyano substituents. The role of bridge-orbital energetics in influencing the electronic coupling in MV bis(triarylamine) compounds has been discussed elsewhere.[27,33]

Plots of ln(k_{ET}) versus $1/T$ for $\mathbf{3}^+$ and $\mathbf{7}^+$ are linear (Figure 4), consistent with an Arrhenius-type temperature dependence of the ET rate, i.e.,

$$k_{ET} = A \exp\left(\frac{-\Delta G^{\ddagger}}{k_B T}\right) \quad (4)$$

where k_B denotes the Boltzmann constant. The barriers to thermal ET extracted from the Arrhenius plots, $\Delta G^{\ddagger}_{ESR}$, are given in Table 1 along with barriers, $\Delta G^{\ddagger}_{NN}$, estimated using eq 3 from parameters obtained from Hush analysis of the IVCT bands (shown in Figure 5), the values of the electronic coupling, V_{NN}, being obtained from eq 2 by equating the diabatic ET distance, R, to the N—N separation, R_{NN}. The ET barriers, $\Delta G^{\ddagger}_{NN}$, estimated from optical data are considerably higher than the values obtained from the VT-ESR data. Similar differences are obtained between optical and VT-ESR rate data for a bis(triarylmethyl) radical anion isoelectronic with $\mathbf{7}^+$.[11,16,64] Using the VT-ESR barriers, $\Delta G^{\ddagger}_{ESR}$, and the optical values of λ, eq 3 affords alternative estimates of the coupling, V_{ESR}, in $\mathbf{3}^+$ and $\mathbf{7}^+$. From these values of V_{ESR}, along with the optical values of μ_{ge} and E_{op}, values of the diabatic ET distance, R_{ESR}, can be obtained from eq 2; as shown in Table 1, these values imply that R in $\mathbf{3}^+$ and $\mathbf{7}^+$ is less than half the N—N distance. Previous studies of class-III species, for which an alternative optical estimate of V (namely, $V = E_{op}/2$) can be compared with that from eq 2, also indicate that the N—N distance is a poor approximation to the actual diabatic ET distance in bis(triarylamine) MV species with conjugated bridging groups;[37,38,47] this implies that the redox centers cannot be regarded as purely localized on the triarylamines but that bridge-based orbitals make significant contributions. Quantum-chemical estimates of R for class-II and -III bis(triarylamine)s, including $\mathbf{5}^+$ and $\mathbf{6}^+$,[38] also suggest R to be less than the N—N separation. Our results for $\mathbf{3}^+$ and $\mathbf{7}^+$, however, represent the first experimental demonstration for localized class-II bis(triarylamine) MV compounds.

Finally, we turn to the nature of the thermal intramolecular ET processes in $\mathbf{3}^+$ and $\mathbf{7}^+$. Depending on the interplay between the nuclear and electronic frequencies, ET reactions are categorized as adiabatic or nonadiabatic; these two regimes differ in the prefactor, A, which is determined in limiting cases by the dynamic properties of the slower subsystems.[66−69] In a nonadiabatic ET reaction the electronic motion is slower than

(65) In each case the IVCT band was satisfactorily fitted using a symmetrical Gaussian (with an additional variable offset included in the fit to model any non-zero baseline) over the energy range below which overlap with other transitions is evident, as previously reported for $\mathbf{3}^+$ and related species[25,27,35,38] and for $\mathbf{6}^+$. The neutral species, which are present in excess, do not absorb in the wavelength range shown in Figure 5 (see Supporting Information), while the dications are, according to statistical considerations, present only at negligible concentrations. The estimated uncertainties in the transition dipole moments extracted from these spectra, taking into account both the uncertainty in the absorptivity measurement and the uncertainties in fitting the band, and in estimates of V based on these values of μ_{ge} for a given R, are ±5%.

(66) Newton, M. D.; Sutin, N. *Annu. Rev. Phys. Chem.* **1984**, *35*, 437.

the vibrational motion and the prefactor is a function of the electronic coupling:

$$A_{nad} = V^2 \sqrt{\frac{4\pi^3}{h^2 \lambda k_B T}} \quad (5)$$

where h is Planck's constant. In the adiabatic regime, the vibrational motion is slower than the electronic motion and

$$A_{ad} = \nu_n \quad (6)$$

where ν_n is the nuclear frequency of crossing the barrier. ESR estimates for the preexponential factors, A_{ESR}, for $\mathbf{3}^+$ and $\mathbf{7}^+$, obtained from the fits of the rate data to eq 4, are included in Table 1. While these prefactors are somewhat low compared to the range of expected values for solvent reorientation frequencies ($\nu_n \approx 10^{11}-10^{12}$ s^{-1}),[5,70] they are much lower than those obtained by inserting the values of V_{NN} (or V_{ESR}) and λ from Table 1 into eq 5 ($10^{13}-10^{14}$ s^{-1}), indicating that the ET reactions in bis(triarylamine) MV compounds of this type fall in the adiabatic regime, as expected from classical ET theory. Since high-frequency intramolecular vibrations could also contribute to ν_n, the values of A_{ESR} are smaller than first anticipated. Indeed, prefactors obtained from Arrhenius fits to published VT rate data for a variety of organic MV cations generally fall in the range of $10^{11}-10^{12}$ s^{-1}.[7-9,43,44] However, there are organic MV precedents for prefactors of the magnitude found for $\mathbf{3}^+$ and $\mathbf{7}^+$; in particular, a very similar value of 3×10^{10} s^{-1} can be derived for a bis(triarylmethyl) radical anion, an anion which is structurally analogous to $\mathbf{7}^+$, in CH_2Cl_2.[11,16]

Conclusion

The intramolecular ET rates in bis(triarylamine) MV radical cations depend on the length of the bridging group, linkage by ethynylene vs vinylene groups, and substitution of bridging phenylene groups, as is expected from electronic couplings and reorganization energies obtained from optical data. Radical cations $\mathbf{3}^+$ and $\mathbf{7}^+$ are the first triarylamine MV species for which ESR spectra have been found to exhibit a temperature-dependent transition from the slow to fast régime and in which optical and thermal ET have been observed and correlated. Comparison of the thermal ET barriers obtained from ESR measurements with those estimated from optical data indicates that the diabatic ET distance in class-II MV triarylamine species with conjugated bridging groups is considerably less than the N—N separation, while the VT-ESR data also indicate that the ET in these compounds is adiabatic. Thus, VT-ESR studies afford a deeper insight into the charge (de)localization and intramolecular ET phenomena in amine-based MV compounds.

Experimental Section

General. The following compounds were synthesized as previously described: **1**,[24] **2**,[25] **3**,[25] **5**,[37] and **6**.[38] Solvents were dried by passing through columns of activated alumina in a manner similar to that described in the literature.[71] Silica gel for chromatography was purchased from Sorbent Technologies (60 Å, 32−63 μm). Elemental analyses were performed by Atlantic Microlabs. Electrochemical measurements were carried out under nitrogen on dry deoxygenated dichloromethane solutions ca. 10^{-4} M in analyte and 0.1 M in tetra-*n*-butylammonium hexafluorophosphate using a BAS potentiostat, a glassy carbon working electrode, a platinum auxiliary electrode, and, as a pseudoreference electrode, a silver wire anodized in 1 M aqueous potassium chloride. Potentials were referenced to ferrocenium/ferrocene by using cobaltocenium hexafluorophosphate (−1.32 V vs ferrocenium/ferrocene) as an internal standard.

4-[Bis(4-*n*-butoxyphenyl)amino]benzaldehyde, 8. 4-Bromobenzaldehyde (17.7 g, 95.7 mmol) was added to a solution of tris(dibenzylideneacetone)dipalladium(0) (0.44 g, 0.48 mmol) and 1,1′-bis(diphenylphosphino)ferrocene (0.40 g, 0.72 mmol) in dry toluene (150 mL) under nitrogen. After 15 min of stirring, sodium *tert*-butoxide (8.59 g, 89.3 mmol) and di(4-*n*-butoxyphenyl)amine (20.0 g, 63.8 mmol, prepared as previously described[47]) were added. The reaction mixture was heated to 90 °C for 24 h. After the reaction mixture was allowed to cool to room temperature, water was added, and the reaction mixture was extracted with diethyl ether. The product was purified by column chromatography (silica gel, 1:9 ethyl acetate/hexane) to give a yellow oil (22.2 g, 83%). ^{1}H NMR (300 MHz, CD_2Cl_2) δ 9.76 (s, 1H), 7.63 (d, $J = 8.8$ Hz, 2H), 7.15 (d, $J = 8.8$ Hz, 4H), 6.92 (d, $J = 8.8$ Hz, 4H), 6.84 (d, $J = 8.8$ Hz, 2H), 3.97 (t, $J = 6.4$ Hz, 4H), 1.77 (m, 4H), 1.01 (t, $J = 7.4$ Hz, 6H). ^{13}C{^{1}H} NMR (75 MHz, CD_2Cl_2) δ 190.2, 157.5, 154.5, 139.0, 131.5, 128.6, 128.2, 116.8, 116.0, 68.5, 31.8, 19.7, 14.0. HRMS-FAB (*m*/*z*): [M$^+$] calcd. for $C_{27}H_{31}NO_3$, 417.2304; found, 417.2307.

***E*,*E*-1,4-Bis{4-[di(4-*n*-butoxyphenyl)amino]styryl}-2,5-dicyanobenzene, 7.** To a mixture of tetraethyl-(2,5-dicyano-α,α′-*p*-xylylenediphosphonate)[55] (0.83 g, 1.9 mmol) and **8** (1.62 g, 3.88 mmol) in tetrahydrofuran (15 mL) at 0 °C was added potassium *tert*-butoxide (0.87 g, 7.8 mmol) in THF (10 mL) dropwise. The resultant solution was stirred at 0 °C for 30 min and at room temperature for 4 h. The reaction mixture was then poured into water and extracted into diethyl ether. The ether layer was collected and concentrated by rotary evaporation, and the residue was purified using flash column chromatography on silica using a solution of hexane/dichloromethane (2:1) to give a red solid (1.24 g, 67%). ^{1}H NMR (300 MHz, CD_2Cl_2) δ 7.99 (s, 2H), 7.38 (d, $J = 8.5$ Hz, 4H), 7.23 (d, $J = 16.1$ Hz, 2H), 7.14 (d, $J = 16.1$ Hz, 2H), 7.06 (d, $J = 8.7$ Hz, 8H), 6.85 (d, $J = 8.6$ Hz, 12H), 3.94 (t, $J = 6.5$ Hz, 8H), 1.74 (m, 8H), 1.48 (m, 8H), 0.97 (t, $J = 7.4$ Hz, 12H). ^{13}C{^{1}H} NMR (CD_2Cl_2, 75 MHz) δ 156.6, 150.4, 140.2, 138.9, 134.5, 129.6, 128.6, 127.7, 127.4, 119.3, 118.8, 117.3, 115.8, 114.7, 68.4, 31.8, 19.7, 14.1. HRMS-FAB (*m*/*z*): [M$^+$] calcd for $C_{64}H_{66}N_4O_4$, 954.50841; found, 954.50717. Anal. Calcd for $C_{64}H_{66}N_4O_4$: C, 80.47; H, 6,96; N, 5.87; found: C, 80.42; H, 6.98; N, 5.94. Cyclic voltammatry (0.1 M $[^nBu_4N]^+[PF_6]^-$ in CH_2Cl_2): $E_{1/2}$ +0.26 ($\mathbf{7}^{+/0}$, $\mathbf{7}^{2+/+}$), +0.94 ($\mathbf{7}^{3+/2+}$) V vs $FeCp_2^{+/0}$.

Generation of Radical Cations for Optical and ESR Spectroscopy. Tris(4-bromophenyl)aminium hexachloroantimonate ($E_{1/2}^{+/0} = +0.70$ V vs $FeCp_2^{+/0}$ in CH_2Cl_2[72]) was purchased from Aldrich and used as the oxidant to generate radical cations in situ. To minimize contributions to the optical and ESR spectra from any diamine dication arising from disproportionation, a ca. 10-fold excess of the neutral amine derivative was added to a solution of $[(p\text{-}BrC_6H_4)_3N]^+[SbCl_6]^-$ of known concentration in dichloromethane. Visible-NIR spectra were recorded in 1 cm cells using a Varian Cary 5E spectrometer. ESR spectra were acquired on a Bruker EMX spectrometer in dry CH_2Cl_2 solution. For ESR spectra recorded at room temperature (those shown in Figures 1 and S4), the solutions were ca. 3×10^{-4} M in radical cation and were recorded from samples in 4 mm ESR tubes. A previous study of solutions containing 4,4′-bis[*N*-phenyl-*N*-(*m*-tolyl)amino]biphenyl and its radical cation found that intermolecular ET has little effect on the ESR line shape of bis(triarylamine) radical cations at concentrations of this magnitude.[45] For ESR spectra recorded at

(67) Demadis, K. D.; Hartshorn, C. M.; Meyer, T. J. *Chem. Rev.* **2001**, *101*, 2655.
(68) Brunschwig, B. S.; Creutz, C.; Sutin, N. *Chem. Soc. Rev.* **2002**, *31*, 168.
(69) Coropceanu, V.; André, J. M.; Malagoli, M.; Brédas, J. L. *Theor. Chem. Acc.* **2003**, *110*, 59.
(70) Horng, M. L.; Gardecki, J. A.; Papazyan, A.; Maroncelli, M. *J. Phys. Chem.* **1995**, *99*, 17311.
(71) Pangborn, A. B.; Giardello, M. A.; Grubbs, R. H.; Rosen, R. K.; Timmers, J. F. *Organometallics* **1996**, *15*, 1518.
(72) Connelly, N. G.; Geiger, W. E. *Chem. Rev.* **1996**, *96*, 877.

variable temperatures (those shown in Figures 2 and 3, and the spectra shown in Figure S1), smaller tubes and, therefore, higher concentrations were required for technical reasons. Solutions were ca. 3×10^{-3} M in radical cation and were obtained from samples in 2 mm ESR tubes supported inside 4 mm ESR tubes. In the case of $\mathbf{3}^+$ and $\mathbf{7}^+$, the high-concentration room-temperature spectra are very similar to those obtained at lower concentration, indicating the effect of intermolecular ET can be neglected. In the case of $\mathbf{2}^+$ and $\mathbf{6}^+$, however, the room-temperature spectra at higher concentration are narrowed and show less well-resolved coupling relative to the low concentration sample, presumably indicating some influence from intermolecular ET. In the fast limit, intermolecular ET is expected to lead to a narrow Lorentzian line shape and loss of hyperfine coupling.[45]

Quantum-Chemical Calculations. The geometries of the *delocalized* radical cations of **1**−**7** were optimized at the spin-unrestricted density functional theory (DFT) level with the B3LYP hybrid functional and the 6−31G(d,p) split-valence plus polarization basis set. The ^{n}Bu groups of $\mathbf{7}^+$ were simplified as Me groups for the calculations. This level of computation gives hyperfine coupling values in good agreement with those obtained from ESR spectra for class-III bis(diarylamine) MV compounds.[47] Since DFT is known to overdelocalize an unpaired electron and is, therefore, unsuitable for modeling class-II bis(triarylamine) radical cations directly,[73] the "half"-compounds $\mathbf{1}^+$ and $\mathbf{4}^+$ were used to model the instantaneous localization of charge on one triarylamine. The hyperfine coupling values computed for $\mathbf{1}^+$ and $\mathbf{4}^+$ (see the Supporting Information) were used as initial inputs in the simulation of the experimental VT-ESR spectra. All DFT calculations were performed with the Gaussian03 suite of programs.[74]

Simulation of ESR Spectra. ESR spectra were simulated using the WinSim program[75,76] or the ESR-EXN program[62,63] assuming static delocalization or broadening due to intramolecular ET, respectively. Room-temperature ESR spectra of all compounds and corresponding simulations using both approaches are given in the Supporting Information, along with the parameters used in these simulations and those used in the simulation of the VT-ESR spectra for $\mathbf{3}^+$ and $\mathbf{7}^+$.

Acknowledgment. We thank the National Science Foundation for support through the Science and Technology Center (DMR-0120967) and CRIF (CHE-0443564) Programs, A. Astashkin and D. Jensen for help acquiring ESR spectra, and K.P. Schultz and S.F. Nelsen for help with simulations.

Supporting Information Available: Complete ref 74; VT-ESR spectra for $\mathbf{2}^+$ and $\mathbf{6}^+$; details of DFT-calculated hyperfine coupling constants; comparison of simulated and experimental room-temperature spectra of all compounds; parameters used in ESR simulations; UV−vis absorption spectra of neutral **3** and **7**; and absolute energies and coordinates of all calculated structures. This material is available free of charge via the Internet at http://pubs.acs.org.

JA808465C

(73) For an overview of the self-interaction error, see: Koch, W.; Holthausen, M. C. *A Chemist's Guide to Density Functional Theory*, 2nd ed.; Wiley-VCH: Weinheim, 2002.

(74) Frisch, M. J.; et al. *Gaussian 03*, revision B.02; Gaussian, Inc., Pittsburgh, PA, 2003.

(75) Duling, D. R. *J. Magn. Reson. Ser. B* **1994**, *104*, 105.

(76) http://www.niehs.nih.gov/research/resources/software/tools/index.cfm.